BY-NC

Mirosław Łomozik

# Structure and plastic properties of HAZ area in 13HMF steel after over 130 000 hours of operation while subjected to simulation welding thermal cycles

**Abstract:** Structural CGHAZ, FGHAZ, ICCGHAZ and SRCGHAZ areas in the heat affected zone (HAZ) of welded joints are characterised. On the basis of simulation, in steel 13HMF after a long-lasting operation different HAZ areas were simulated in conditions imitating the effect of multiple welding thermal cycles (multilayer welding). Results of plastic properties (impact energy and hardness) tests as well as microstructure examination of individual simulated HAZ areas in 13HMF steel have been discussed.

**Keywords**: welding, 16HMF steel, Thermal Cycles;

## Introduction

Steel 13HMF belongs to an older generation of steels used at heightened temperatures and intended for the production of critical power engineering structures, particularly for welded structures. Despite many years of presence on the domestic and overseas markets, the steel continues to be used in the production of power engineering systems (according to DIN regulations steel 13HMF is designated as 14MoV63).

Presently, due to wear, welded structures such as welded power generation systems are susceptible to failures, which should also be expected in the future. The most convenient solution would be to completely replace old structures with new ones. However, due to technical or economic reasons such a solution is often unfeasible and must be substituted with repair of welded structures. The issue of the operation of power engineering-related welded structures, including those made of steel 13HMF, was extensively addressed within the confines of international research project COST 538, the main objective of which was High Temperature Plant Lifetime Extension.

During a welding process, the areas of a base metal adjacent to a weld become heated to high temperatures, significantly over the temperature AC3, and then cool at various rates. The area of a material being welded in which welding thermal cycles cause the changes of the structure and properties of this material is referred to as the Heat Affected Zone (HAZ). The changes in the structure and properties of HAZ result from allotropic and structural (phase) changes as well as deformations of the crystallographic lattice taking place in the material being welded. Depending on the physicochemical properties of a material the changes referred to above may occur separately or simultaneously.

dr hab. inż. Mirosław Łomozik (PhD Eng.), professor extraordinary at Instytut Spawalnictwa in Gliwice, Testing of Materials Weldability and Welded Constructions Department

BY-NC

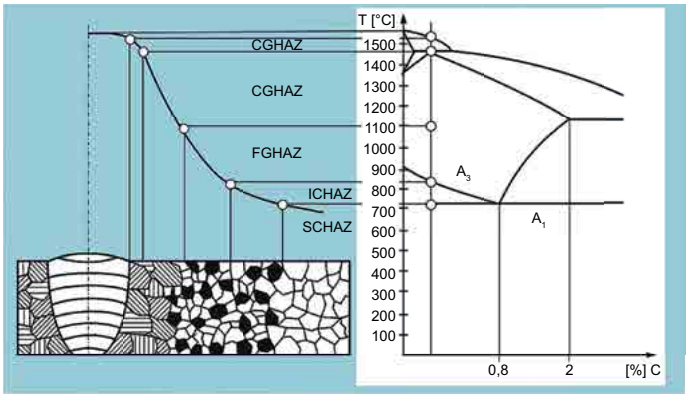


Fig. 1. Distribution of structural areas in HAZ of low--alloy steel in function of temperature, in relation to iron-carbon phase equilibrium system [1- 8]

In metals undergoing allotropic changes or phase changes in the solid state the HAZ area is not homogenous but reveals several areas characterised by different morphology as well as mechanical and plastic properties. Such a type of HAZ is present in welded joints made of low-carbon structural steels or low-alloy structural steels. The distribution of the areas in the HAZ of a welded joint made of low-alloy steel is presented in Figure 1.

The symbols in Figure 1 denote the following respectively [6, 9-12]:

- **CGHAZ** (Coarse Grained HAZ) – HAZ area characterised by a coarse grained structure ($T_{max} \geq 1150°C$),
- **FGHAZ** (Fine Grained HAZ) - HAZ area characterised by a fine grained structure, heated to a temperature above $A_{C3}$ ($900 \leq T_{max} < 1150°C$),
- **ICHAZ** (Intercritical HAZ) - HAZ area heated to a temperature within the range $A_{C1} \div A_{C3}$ ($700 \leq T_{max} < 900°C$),
- **SCHAZ** (Subcritical HAZ) - HAZ area heated to a temperature below $A_{C1}$ ($600 \leq T_{max} < 700°C$).

Examples of microstructure changes in various areas of a real welded joint made of unalloyed steel undergoing structural changes are presented in Figure 2.

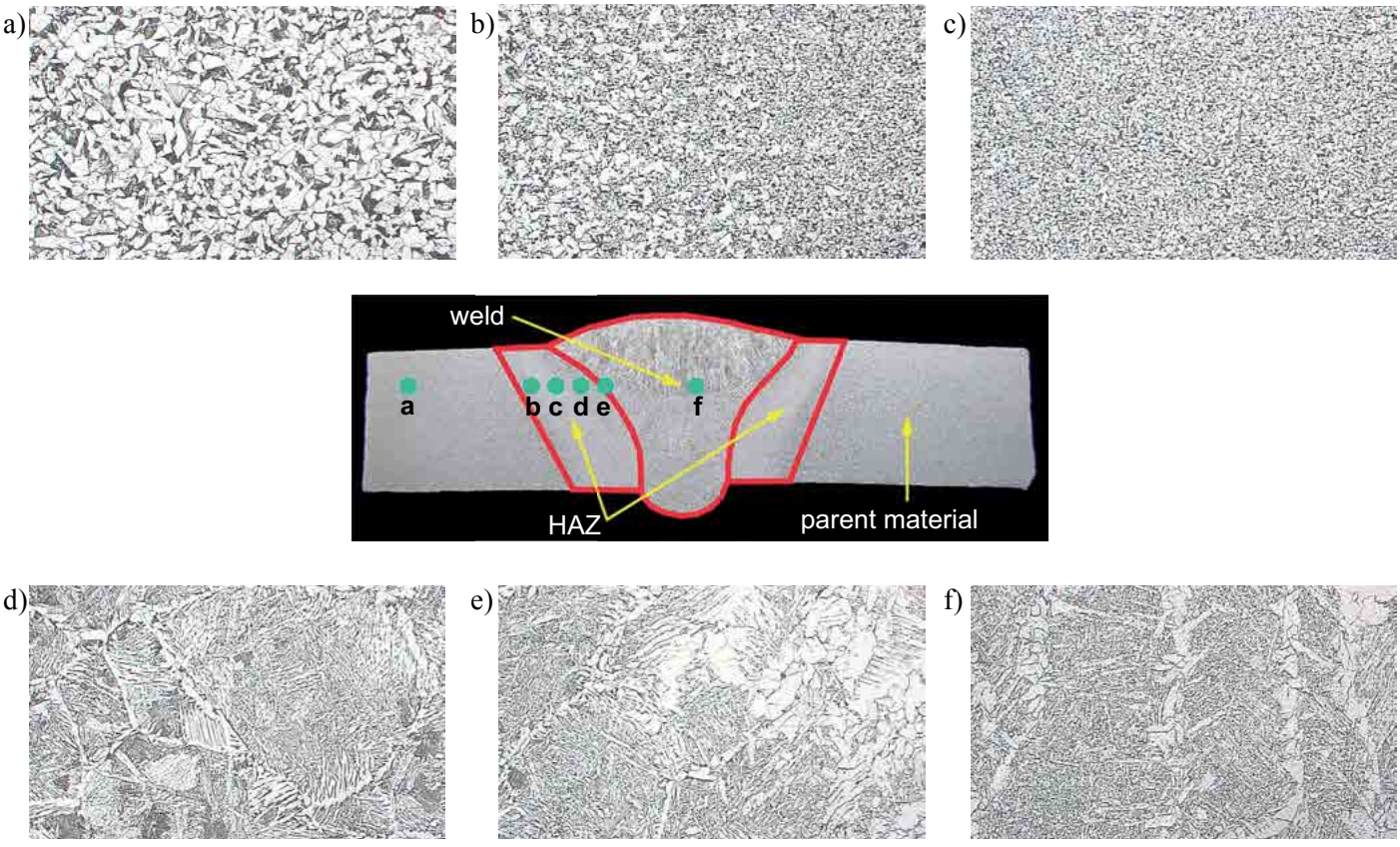


Fig. 2. Example of microstructure changes in various areas of welded joint made of unalloyed steel: a) base metal, ferrite + pearlite, b) ICHAZ area, fine grained ferritic-pearlitic structure with diverse-sized ferrite grain, c) FGHAZ area, homogenous and fine grained ferritic-pearlitic structure, d) CGHAZ area, Widmanstätten pattern, e) transition zone between HAZ and weld, f) weld, bainite + granular ferrite located on former austenite grain boundaries

BY-NC

In steels with a higher carbon content (above 0.25%) and in steels containing small amounts of alloying elements the structure of the HAZ area is close to the morphology of the HAZ in welded joints made of low-carbon steels. A characteristic feature of the HAZ area in joints made of steel with a greater carbon content and in low-alloy steels is the presence of hardening structures such as martensite and bainite. This results from the increased hardenability of these groups of steels if compared with low-carbon steels. In the case of these steels hardening structures are mainly present in the CGHAZ (Coarse Grained HAZ).

During multi-pass welding, while making next runs (layers) of a weld, the HAZ area is affected by successive thermal cycles leading to the formation of metallographic structures characterised by various plastic properties. In addition, during multi-pass welding in the HAZ it is possible to observe the formation of tempered structure zones. In their research, Toyoda [10] and Kiefer [13] noticed that during multi-pass welding successive thermal cycles affect not only the structure and properties of individual runs (layers) of a weld but also the properties of the HAZ of a joint. The authors state that the formation of tempered microstructure zones in the HAZ area reduces hardness and decreases plastic properties, particularly toughness.

The area of the most disadvantageous plastic properties is the coarse grained HAZ (CGHAZ). During multi-pass welding certain regions of the CGHAZ area become reheated to an intercritical temperature within the range $A_{C1} \div A_{C3}$ and, as a result, after cooling it is possible to observe an intercritically reheated Coarse Grained HAZ area (ICCGHAZ) characterised by equally low or even lower plastic properties than those of the CGHAZ. On one hand, in order to increase the efficiency of a welding process it is desirable to increase the amount of heat supplied to a joint. On the other hand, however, an increase in the amount of heat supplied to a joint deteriorates the plastic properties of the coarse grained HAZ [13]. At the same time, in the case of greater thicknesses of elements, multi-pass welding is inevitable, which in turn leads to overlapping of thermal cycles and in consequence, to the formation of ICCGHAZ in the HAZ area. For these reasons, the main objective of the tests was to determine the impact of welding thermal cycles on impact energy, hardness and structure of various simulated HAZ areas in steel 13HMF in the state following long-lasting operation.

## Material used in the tests

The tests involved the use of steel 13HMF in the state following long-lasting operation of 132 782 hours' duration, at a temperature of approximately 540°C and under a pressure of approximately 18 MPa. The chemical composition of the steel tested is presented in Table 1, whereas its mechanical properties at ambient temperature and heightened temperatures are presented in Table 2.

The values of critical temperatures $A_{C1}$ and $A_{C3}$ of the tested steel 13HMF were determined using the following equations [15, 16]:

Table 1. Chemical composition of steel 13HMF after long-lasting operation

| Steel grade | Chemical element content, % | | | | | | | | | | |
|---|---|---|---|---|---|---|---|---|---|---|---|
| | C | Mn | Si | P | S | Cr | Ni | Mo | V | Cu | Al |
| 13HMF | 0,15 | 0,49 | 0,29 | 0,025 | 0,012 | 0,36 | 0,04 | 0,59 | 0,26 | 0,016 | <0,005 |
| acc. to PN-75/H-84024 [14] | 0.1 ÷ 0.18 | 0.40 ÷ 0.70 | 0.15 ÷ 0.35 | max 0.040 | max 0.040 | 0.30 ÷ 0.60 | max 0.30 | 0.50 ÷ 0.65 | 0.22 ÷ 0.35 | max 0.25 | max 0.020 |

BY-NC

$$A_{C1} = 723 - 10{,}7 \cdot Mn - 16{,}9 \cdot Ni + 29{,}1 \cdot Si + 16{,}9 \cdot Cr + 290 \cdot As + 6{,}38 \cdot W \quad (1)$$

$$A_{C3} = 910 - 203 \cdot C^{1/2} - 15{,}2 \cdot Ni + 44{,}7 \cdot Si + 104 \cdot V + 31{,}5 \cdot Mo + 13{,}1 \cdot W - (30 \cdot Mn + 11 \cdot Cr + 20 \cdot Cu - 700 \cdot P - 400 \cdot Al - 120 \cdot As - 400 \cdot Ti) \quad (2)$$

After entering chemical element contents from Table 1 into equations (1) and (2) the following values of critical temperatures of steel 13HMF were obtained: $A_{C1}$=732°C and $A_{C3}$=890°C.

Table 2. Results of steel 13HMF static tensile test after operation at ambient temperature and heightened temperatures

| Steel | Testing temperature, °C | Mechanical properties | | Plastic properties | |
|---|---|---|---|---|---|
| | | $R_{0.2}$, Mpa | $R_m$, MPa | $A_5$, % | Z, % |
| 13HMF | 20 | 411.4 | 583.1 | 23.5 | 76.0 |
| | 200 | 319.3 | 494.7 | 21.3 | 75.7 |
| | 300 | 322.0 | 512.0 | 21.2 | 74.5 |
| | 350 | 317.0 | 471.0 | 22.0 | 77.7 |
| | 400 | 334.0 | 427.0 | 17.7 | 80.6 |
| | 450 | 306.0 | 380.0 | 22.3 | 82.8 |
| | 500 | 264.0 | 309.0 | 23.6 | 87.4 |
| | 550 | 236.5 | 274.5 | 28.4 | 89.8 |
| acc. to PN-75/H-84024 [14] | | min. 363 | min. 491 | min. 18 | - |

Table 3. Parameters of simulated thermal cycles for various HAZ areas of steel 13HMF.

| HAZ area | $T_{max}$, °C | | | Cooling time $t_{8/5}$, s | | | | |
|---|---|---|---|---|---|---|---|---|
| | $T_{max1}$ | $T_{max2}$ | $T_{max3}$ | 6 | 12 | 24 | 60 | 120 |
| CGHAZ | 1250 | - | - | × | × | × | × | × |
| FGHAZ | 1250 | 950 | - | × | × | | × | |
| ICCGHAZ | 1250 | 800 | - | × | × | | × | |
| SRCGHAZ | 1250 | 700 | - | × | × | | × | |
| Temper bead cycle | 1250 | 720 | 550 | × | | × | × | |

Where:
- CGHAZ – HAZ area corresponding to coarse grained superheated area,
- FGHAZ – corresponds to the fine grained HAZ area reheated to a temperature above $A_{C3}$,
- ICCGHAZ – corresponds to the coarse grained HAZ area reheated to a temperature in the intercritical range $A_{C1} \div A_{C3}$,
- SRCGHAZ – corresponds to the coarse grained HAZ area reheated to a temperature $A_{C1}$,
- Temper bead cycle – corresponds to the superheated coarse grained HAZ area subjected to a tempering cycle,
- $t_{8/5}$ – cooling time of steel HAZ area in the temperature range between 800 and 500°C.

## Simulating multiple welding thermal cycles

The steel tested was used for preparing samples for the simulation of welding thermal cycles. The samples had a shape, dimensions and Charpy V-notch appropriate for testing impact energy.

Afterwards, a simulator of thermal-strain cycles was used to carry out tests aimed to simulate multiple welding thermal cycles in HAZ area samples of various structures and properties. The scheme of simulation is presented in Table 3.

In cases when due to technical reasons the carrying out of a conventional post-weld heat treatment is limited or impossible (e.g. during repair welding), a solution which may enable obtaining appropriate plastic properties of the HAZ area is the use of temper beads during welding.

A temper bead technique consists in such a manner and sequence of making individual beads of a weld so that a controlled welding thermal cycle could lead to the tempering of the hardening structures in the areas of previously made beads both in the weld and in the HAZ of welded steel.

## Test results [17]

The samples with simulated HAZ areas were used in impact energy tests in accordance

BY-NC

with the requirements of standard PN-EN ISO 148-1 [18]. The tests were carried out at ambient temperature. A criterion provided in standard PN-EN 12952-6 [19] specifies the minimum value of the impact energy for samples with a normal cross-section (10×10 mm) in the HAZ at 24 J at the ambient temperature, whereas standard PN-EN 10216-2 [20] specifies the minimum value of the impact energy for the base metal at 27 J. The criteria-related values of impact energy are presented in figures showing test results.

From each series of the samples simulated with various welding thermal cycles one

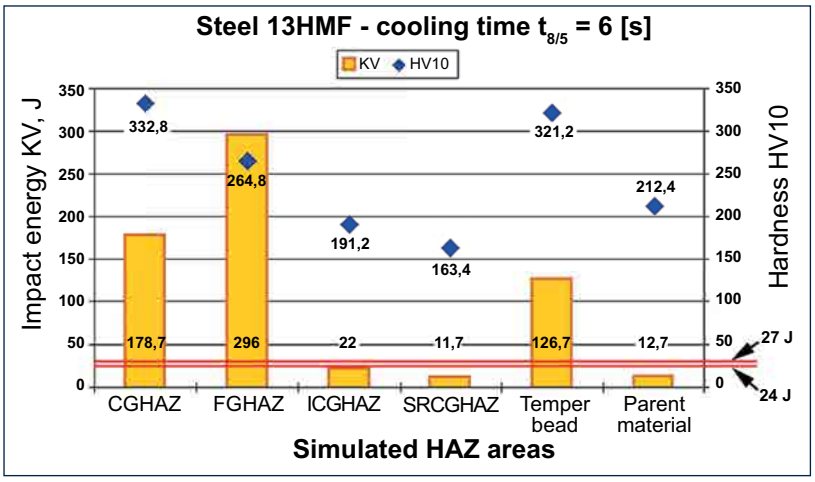


Fig. 3. Comparison of impact energy KV and hardness HV10 of various HAZ areas of steel 13HMF for cooling time $t_{8/5}$ = 6 s

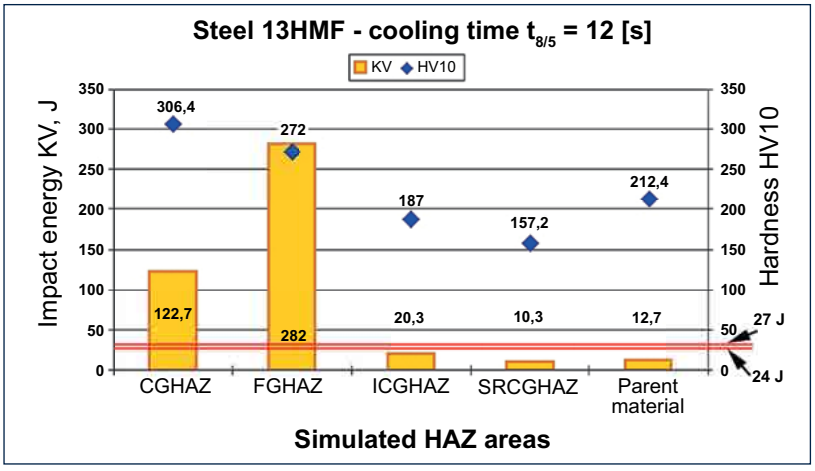


Fig. 4. Comparison of impact energy KV and hardness HV10 of various HAZ areas of steel 13HMF for cooling time $t_{8/5}$ = 12 s

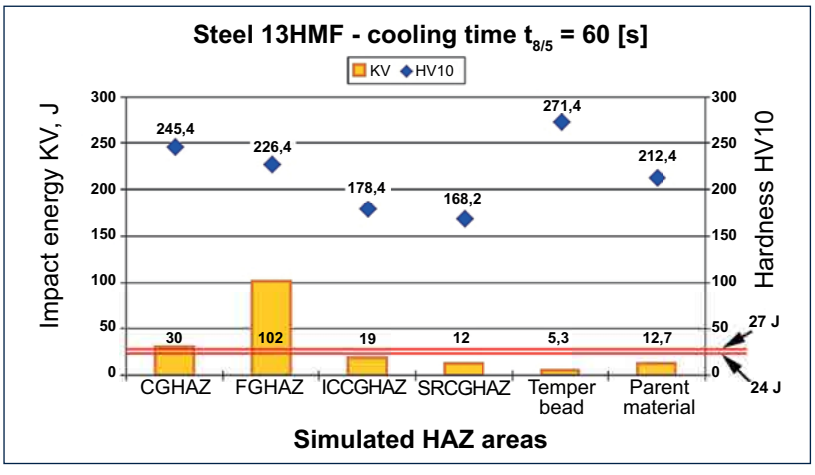


Fig. 5. Comparison of impact energy KV and hardness HV10 of various HAZ areas of steel 13HMF for cooling time $t_{8/5}$ = 60 s

Fig. 6. Base metal of steel 13HMF after 132 782 hours' operation. Ferrite + bainite + fine dispersive carbides inside grains. Hardness: 212.4 HV10

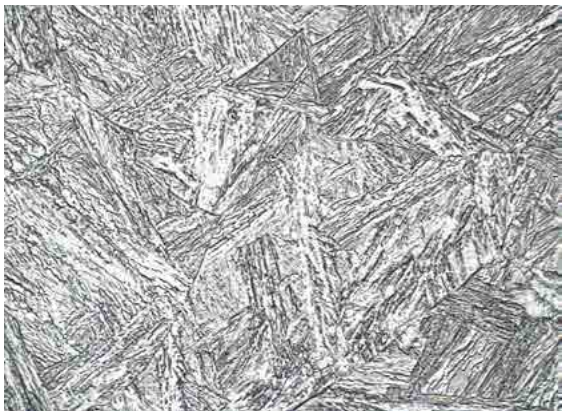

Fig. 7. CGHAZ area ($T_{max}$ = 1250°C, $t_{8/5}$ = 6 s). Bainite + martensite. Hardness: 332.8 HV10

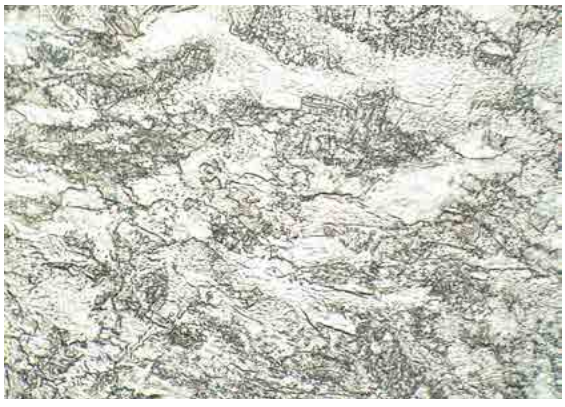

Fig. 8. FGHAZ area ($T_{max}$ = 1250+950°C, $t_{8/5}$ = 6 s). Bainite + granular ferrite. Hardness: 264.8 HV10

BY-NC

sample was selected for microscopic metallographic tests. On sample surfaces perpendicular to the plane in which an impact test notch was cut, metallographic specimens were made in accordance with the requirements of standard PN-EN 1321 [21]. The microstructure of the samples was revealed with the Nital etchant. The metallographic specimens were used for hardness measurements of individual simulated HAZ areas. Measurements were conducted with the Vickers method under a load of 98.07 N (HV10) in accordance with the requirements of standard PN-EN ISO 6507-1 [22]. The selected examples of impact energy test results and hardness measurements of the individual areas of the simulated HAZ of steel 13HMF are presented in Figures 3-5.

The examples of metallographic microscopic tests results at magnification 1000x are presented in Figures 6-11.

Fig. 9. ICCGHAZ area ($T_{max}$ = 1250 + 800°C, $t_{8/5}$ = 6 s). Ferrite + pearlite. Hardness: 191.2 HV10

Fig. 10. SRCGHAZ area ($T_{max}$ = 1250 + 700°C, $t_{8/5}$ = 6 s). Ferrite + pearlite. Hardness: 163.4 HV10

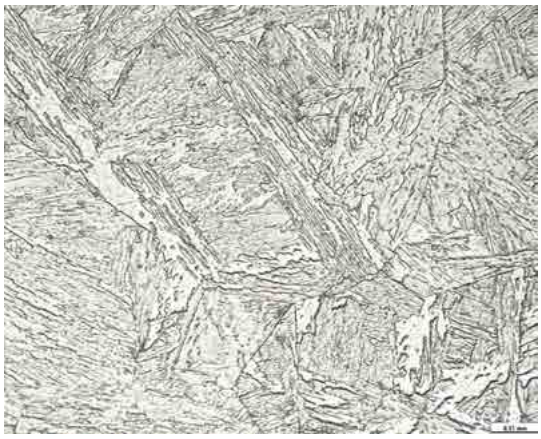

Fig. 11. HAZ area after tempering cycle ($T_{max}$ = 1250 + 720 + 550°C, $t_{8/5}$ = 6 s). Bainite. Hardness: 321.2 HV10

## Summary

The initial state adopted was the structure and properties of steel 13HMF after long-lasting operation of 132 782 hours. The impact energy in the initial state at ambient temperature was low and amounted to mere 12.7 J. This state was mainly caused by creeping processes and numerous fine dispersive carbide precipitates located inside grains in the steel structure. The hardness in the initial state amounted to 212.4 HV10.

In the HAZ area obtained after single heating with a thermal cycle of a maximum temperature amounting to 1250°C (CGHAZ) along with the extension of a cooling time, an impact energy decreases from 178.7 J for $t_{8/5}$ = 6 seconds to 30 J for $t_{8/5}$ = 60 seconds. For the same range of cooling times hardness changes from 332.8 HV10 to 245.4 HV10. The microstructure of the CGHAZ area evolves from the mixture of bainite and martensite and bainite and ferrite for short and medium cooling times up to the mixture of bainite and coarse precipitates of granular ferrite for long cooling times $t_{8/5}$. The reason for such a significant decrease in the impact energy of this HAZ area is an increasing amount of granular ferrite located on former austenite grain boundaries.

BY-NC

The HAZ area of a fine grained structure (FGHAZ) was obtained after double heating with a thermal cycle – first to a maximum temperature of 1250°C and next to a temperature of 950°C. The impact energy of this HAZ area is very high for very short cooling times and amounts to 296 and 282 J for dla $t_{8/5}$ = 6 seconds and 12 seconds respectively. In the case of a time $t_{8/5}$ = 60 seconds it is possible to observe a decrease in impact energy to a value of 102 J. Such a situation is caused by the growth of grain sizes in the steel microstructure composed of the mixture of granular ferrite and bainite which in turn is due to a longer time at which the HAZ material remains at a temperature above $A_{C3}$.

The coarse grained HAZ - ICCGHAZ – was obtained as a result of double heating with a thermal cycle, where the second cycle included heating to a maximum temperature contained in the range of critical temperatures $A_{C1} \div A_{C3}$. The impact energy of the HAZ changes from 22 J for $t_{8/5}$ = 6 seconds to 19 J for $t_{8/5}$ = 60 seconds, which indicates that extending a cooling time has practically no effect on the value of impact energy of this HAZ area, in which impact energy is generally low. The microstructure of the ICCGHAZ area is composed of a mixture of ferrite and pearlite. The hardness changes from 191.2 HV10 to 178,4 HV10.

In the coarse grained HAZ area obtained after reheating with a thermal cycle to a maximum temperature of 700°C (SRCGHAZ), which was slightly lower than the temperature $A_{C1}$, the character of impact energy changes is similar to that of the ICCGHAZ area. The values of impact energy change from 11.7 J for $t_{8/5}$ = 6 seconds to 12 J for $t_{8/5}$ = 60 seconds. In turn, hardness changes from 163.4 HV10 to 168.2 HV10 for analogous values of cooling times. It can be seen that a change of cooling time $t_{8/5}$ does not significantly affect impact energy or hardness changes. It is also possible to observe that both impact energy and hardness for individual cooling times are lower than the impact energy and hardness of the base metal of steel 13HMF. In general, the impact energy of the SRCGHAZ area is low. Independent of cooling time $t_{8/5}$ the microstructure of the SRCGHAZ area is characterised by the mixture of granular ferrite and pearlite.

The HAZ area after a tempering cycle was subjected to a triple thermal cycle, where the first cycle included heating to a maximum temperature of 1250°C, the second one to a temperature of 720°C (slightly lower than temperature $A_{C1}$), and the third one to a temperature of 550°C. As a result of a tempering cycle, for a cooling time $t_{8/5}$ = 6 seconds, a clearly visible improvement of impact energy in comparison with the base metal was obtained. For a cooling time $t_{8/5}$ = 6 seconds the impact energy amounts to 126.7 J (almost 10 times greater if compared with the initial state). For a cooling time $t_{8/5}$ = 60 seconds the impact energy amounts to mere 5.3 J. Such a phenomenon is caused by an increasing amount of coarse granular ferrite in the steel microstructure. The microstructure of the HAZ area after a tempering cycle changes from a bainitic-martensitic structure for short cooling times to a mixture of bainite and granular ferrite for longer cooling times.

## Conclusions

On the basis of the tests conducted it is possible to state the following

1. Steel grade 13HMF after long-lasting operation has a chemical composition consistent with the requirements of a related metallurgical standard.

2. In the coarse grained areas ICCGHAZ and SRCGHAZ of steel 13HMF after long-lasting operation, cooling time $t_{8/5}$ has practically no effect on changes of the impact energy and hardness as well as on the microstructure of these HAZ areas.

BY-NC

3. In the tested steel 13HMF, the impact energy of ICCGHAZ and SRCGHAZ areas is low (approximately 20 J and 10÷12 J respectively) and comparable with the impact energy of this steel in the initial state (12,7 J).

4. In steel 13HMF, after long-lasting operation, the impact energy of the HAZ area after a tempering cycle for a cooling time $t_{8/5}$ = 6 seconds is significantly higher than the impact energy of the simulated ICCGHAZ and SRCGHAZ areas, i.e. the areas reheated to a temperature in the range of $A_{C1}$÷$A_{C3}$ and to a temperature lower than AC1 respectively.

5. In relation to the tested steel 13HMF, when it is not possible to perform a post-weld treatment or revitalisation, a practical manner of improving the plastic properties of the coarse grained ICCGHAZ and SRCGHAZ areas may be subjecting them to tempering thermal cycles for short cooling times $t_{8/5}$, e.g. 6 seconds.

## References


1. Welding Handbook, Eight Edition, Volume 1, Welding Technology, Chapter 4: Welding metallurgy, American Welding Society, 1987.
2. Seliger, P. and Gampe U. (2002). Life Assessment of Creep Exposed Components, New Challenges for Condition Monitoring of 9Cr Steels. *OMMI*, 1 (2).
3. Radaj, D. (1992). *Heat Effects of Welding. Temperature Field, Residual Stress, Distortion*. Springer - Verlag, Berlin Heidelberg: Springer-Verlag.
4. Pierożek, B. and Lassociński, J. (1987). *Spawanie łukowe stali w osłonach gazowych*. Warszawa: Wydawnictwa Naukowo-Techniczne.
5. Brózda, J., Pilarczyk, J. and Zeman, M. (1983). S*pawalnicze wykresy przemian austenitu CTPc-S*. Katowice: Wydaw. "Śląsk".
6. Ramirez, J. E. Mishael, S. and Shockley, R. (2005). Properties and Sulfide Stress Cracking Resistance of Coarse-Grained Heat-Affected Zones in V-Microalloyed X60 Steel Pipe. *Welding Journal, Welding Research*, pp. 113-123.
7. Węgrzyn, J. (1990). *Fizyka i metalurgia spawania*. Gliwice: Politechnika Śląska.
8. Pilarczyk, J. and Pilarczyk, J. (1996). *Spawanie i napawanie elektryczne metali.* Katowice: "Śląsk".
9. Haze, T. Aihara, S. *Metallurgical Factors Controlling HAZ Toughness in HT50 Steels*. IIW Doc. IX-1423-86.
10. Toyoda, M. Minami, F. Yamaguchi, Y. Amano, K. and Kawabata, F. *Tempering Effect on HAZ Toughness of Multi-layered Welds*. IIW Doc. X-1193-89.
11. *Guide to Weldability and Metallurgy of Welding of Steels Processed by Thermomechanical Rolling or by Accelerated Cooling*. IIW Doc. IX-1649-91.
12. Devillers, L. Kaplan, D. and Testard P. (1995). Predicting the microstructure and toughness of weld HAZs. *Welding International*, (9), pp. 128-138.
13. Kiefer, J.H. (1995). Bead Tempering Effects on FCAW Heat-Affected Zone Hardness. *Welding Journal Supplement*, 74 (11), pp. 363-367.
14. PN-75/H-84024 S*tal do pracy przy podwyższonych temperaturach. Gatunki*.
15. Mikuła, J. and Wojnar, L. (1996). *Zastosowanie metod analitycznych w ocenie spawalności stali.* Kraków: Fotobit.
16. Zeman, M. (1987). *Analiza stanu zagadnienia i ukierunkowanie badań wraz z praktycznymi przykładami zastosowań metod matematycznych w analizowanym zakresie.* Instytut Spawalnictwa Research Work no. Hc-60 (C-31.3.4), CPBR 7.3 "Techniki spawalnicze"
17. Łomozik M. (2006). *Optymalizacja metod spawania dla napraw i renowacji elementów z żarowytrzymałych stali po długim okresie eksploatacji w polskich elektrowniach i prognozowanie ich trwa-*

BY-NC

*łości.* Annual report of special research programme COST 538 by Instytut Spawalnictwa, Gliwice.
18. PN-EN ISO 148-1:2010 *Metallic materials. Charpy pendulum impact test. Test method*
19. PN EN 12952-6:2011 *Water-tube boilers and auxiliary installations. Part 6: Inspection during construction; documentation and marking of pressure parts of the boiler*
20. PN-EN 10216-2+A2:2009 *Seamless steel tubes for pressure purposes. Technical delivery conditions. Part 2: Non-alloy and alloy steel tubes with specified elevated temperature properties*.
21. PN-EN 1321:2000 *Destructive tests on welds in metallic materials – Macroscopic and microscopic examination of welds*
22. PN-EN ISO 6507-1:2007, *Metalls. Hardness measurements made by Vickers method. Part 1: research method*